Joint Pathology Center

Veterinary Pathology Services

WEDNESDAY SLIDE CONFERENCE 2016-2017

C o n f e r e n c e 14

11 January 2017

CASE I: HSRL-425 (JPC 4075851).

Signalment: 11-year-old, castrated male, Labrador retriever, (*Canis familiaris*).

History: The patient presented six months prior to euthanasia for evaluation of a cardiac arrhythmia and a several month history of intermittent coughing which had become more severe in the two days before initial presentation. An intermittent split P wave was noted on the ECG. Thoracic radiographs revealed a markedly enlarged heart, right atrial enlargement, enlarged pulmonary vessels, and a diffuse broncho-alveolar pattern. Echocardiography showed a space-occupying mass in the left atrium with mitral and tricuspid valve regurgitation. The patient was discharged with furosemide and returned six months later with exercise intolerance and respiratory distress. At that time due to the patient's declining condition the owner elected euthanasia.

Gross Pathology: A 5 x 6 x 8 cm, firm, multinodular mass is present on the proximocaudal aspect of the heart base, resting on the left atrium. On cross section, the mass is highly vascular and has a mottled red-to-brown mosaic pattern. The mass surrounds the pulmonary arteries, compressing the left pulmonary artery, but it is still patent. The mass is proximal to the pulmonary veins that are not compressed. Tumor invasion into the left atrial lumen is characterized by numerous nodular small projections, up to 0.5 cm, covered by intact endocardium. Left atrial luminal size is decreased due to compression by the mass. Mild endocardiosis of the mitral and tricuspid valves is evident. The right ventricle is distended and dilated in addition to an overall enlarged heart.

The abdomen contains 4 liters of sero-sanguinous clear fluid, with another 2 liters of clear creamy yellowish fluid in the

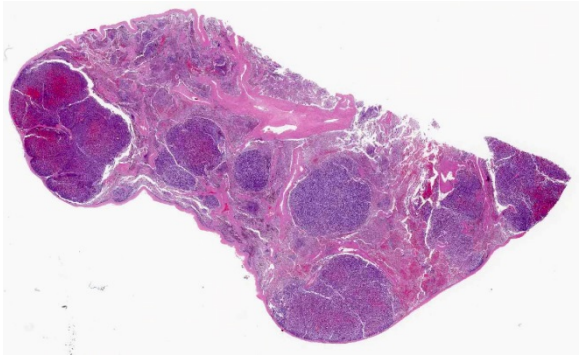

Spleen, dog. The spleen contains numerous well-demarcated neoplastic nodules. (HE, 5X).

thoracic cavity. The spleen has multiple firm white and hemorrhagic masses ranging from 1 mm to 3 cm in size. The consistencies of the splenic masses are similar to the heart mass. The left anterior lung is very pale, soft, and slightly decreased in size due to compression by the left atrial mass. Mediastinal lymph nodes are enlarged with effacement of normal architecture.

Laboratory results: Upon initial presentation, NOVA results are as follows:

- Glucose: 118 mg/dL (60-115)
- Ca++: 1.35 mmol/L (2.2-3.0)
- Mg++: 0.49 mmol/L (1.5-2.5)
- PCO2: 26.1 mmHg (34-40)
- PO2: 49.1 mmHg (85-100)
- SO2: 85.4 % (>90)
- BEecf: -7.3 mmol/L ([0]-[+6])
- nCa: 1.37 mmol/L (1.13-1.33)
- nMg: 0.50 mmol/L (0.26-0.41)

Histopathologic Description: Spleen: There are multiple variably-sized solid nodules effacing and replacing the splenic parenchyma. The neoplastic nodules are well demarcated and expansile. They are composed of large islands of polygonal cells separated by large connective tissue branches and supported by fine fibro-vascular stroma that subdivide the cells in small ribbons. The tumor cells are cuboidal to polyhedral in shape with a round nucleus and a moderate amount of granular lightly amphophilic cytoplasm. The cells are aligned along the small capillaries forming small packets where the cells show polarity with the cytoplasm towards the vessels. Mitotic activity is 11 mitotic figures in 10 hpf. There are areas of marked aniso-karyosis and occasional megalokaryosis (polymorphism) with prominent nucleoli. The large cells show a round eosinophilic prominent nucleolus.

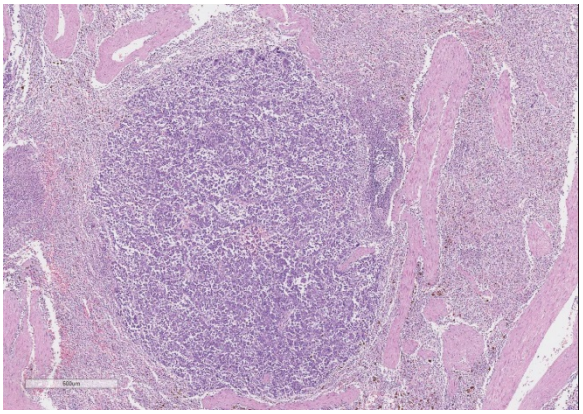

Spleen, dog. Neoplastic nodules are unencapsulated, mildly infiltrative, and neoplastic cells are arranged in nests and packets. (HE, 35X).

The adjacent splenic parenchyma is compressed and attenuated. There are small multiple aggregates of macrophages filled with large granulated golden pigment (hemosiderin- previous hemorrhages). The smooth muscle trabeculae are closer than expected due to collapse of the parenchyma with very few follicles.

Contributor's Morphologic Diagnoses:

1. Heart: Chemodectoma
2. Heart: Mild diffuse mitral and tricuspid valve myxomatous degeneration
3. Spleen: Chemodectoma, metastasis
4. Liver: Chronic severe congestive hepatopathy
5. Lymph Nodes: Chemodectoma, metastasis

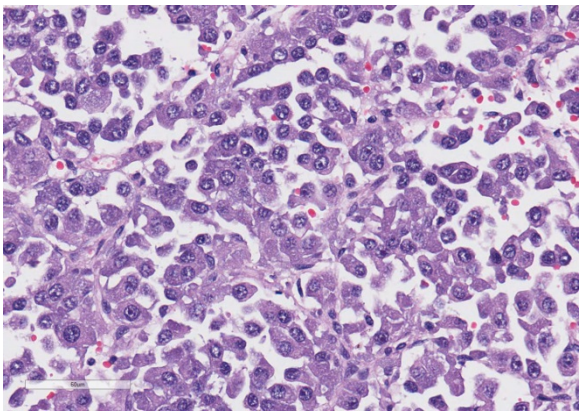

Spleen, dog. Neoplastic cells have granular basophilic cytoplasm with mild variation in nuclear size. (HE, 360X)

Contributor's Comment: Spleen is the only tissue submitted. Chemodectomas are primary neuroendocrine tumors arising most commonly from the chemoreceptor organs of the aortic and carotid bodies.[1,2,4,12] Other chemoreceptors that rarely develop neoplasia include the nodose ganglion of the vagus nerve, ciliary ganglion in the orbit, the pancreas, and the glomus jugulare along the recurrent branch of the glossopharyngeal nerve.[11] They are synonymous with heart base tumors or non-chromaffin, extra-adrenal, paragangliomas in veterinary medicine.[3,4]

Chemodectomas are uncommon neoplasms most often described in canines where they have an incidence of 0.19%.[14] Chemo-dectomas are the second most common cardiac tumor, behind hemangiosarcomas, representing 8% of cardiac tumors.[14] Contrary to humans, aortic body tumors are the more common form of chemodectoma in animals with carotid body tumors being less common and more malignant.[4] In dogs, aortic body tumors are encountered up to four times more frequently than carotid body tumors.[12] The aortic body is located adjacent to the adventitia of the aortic arch at the bifurcation of the subclavian artery while the carotid body is located at the bifurcation of the common carotid artery.[1,4,14] Paren-chymal cells of neuroectodermal origin and sustentacular or stellate cells are the primary cell types that make up the chemoreceptor organs.[4,11] The function of the aortic and carotid bodies is to sense fluctuations in the carbon dioxide, pH, and oxygen tension in blood, which helps to regulate respiration and circulation.[4,7] The aortic and carotid bodies can increase heart rate and elevate arterial blood pressure through the sympathetic nervous system and alter the depth, minute volume, and rate of respiration through the parasympathetic nervous system.[4] The chemoreceptor system is considered part of the parasympathetic nervous system, as it does not secrete catecholamines; however, the presence of secretory granules in the cytoplasm of the glomus cells, the functional cells of chemoreceptors, is inconsistent with this finding.[1,11,12]

Due to the lack of catecholamine production, the tumor's clinical manifestations are the result of being a space-occupying lesion. Smaller adenomas may go undetected, as they can be too small to cause clinical signs, while larger adenomas may press on the atria or displace the trachea and partially surround the major vessels at the base of the heart. Aortic body tumors can also be locally invasive and invade the lumen of the surrounding great vessels or heart chambers hindering blood flow.[4] Common clinical manifestation of aortic body tumors include ascites, pulmonary edema, nutmeg liver, hemothorax, hemopericardium, anasarca, dyspnea, cyanosis, splenomegaly, and arrhythmias.[6,10,12,15] Many of these clinical manifestations are consistent with right-sided congestive heart failure brought on by the tumor acting as a space occupying lesion or by local invasion of vessels resulting in the obstruction of blood flow.[15] Another way aortic body tumors cause lesions is

through metastasis to other parts of the body. It is rare for an aortic body tumor to metastasize, with the most common locations being the lungs and liver.[4] However, other locations have been identified including lymph nodes, myocardium, kidney, adrenal gland, bladder, spleen, and even bone.[4,5,7,12,14] Immunohistochemistry has been valuable to definitively confirm the diagnosis of chemodectomas.[8,12,15]

JPC Diagnosis: Spleen: Neuroendocrine carcinoma, metastatic, Labrador retriever, *Canis familiaris*.

Conference Comment: The contributor provides an excellent summary of the key features of chemodectomas in dogs. As is the tradition at the Joint Pathology Center, conference participants are not provided the full signalment, history, gross necropsy findings, or results of additional histochemical and immunohistochemical stains prior to the conference. Conference participants described nests and packets of neoplastic polygonal cells with small, round, hypochromatic nuclei separated and supported by a delicate fibrovascular stroma, and aptly determined the neoplasm to be of neuroendocrine origin; however, without the additional clinicopathologic information, the site of origin could not be definitively determined from histopathologic evaluation alone. As a result, participants discussed the most likely sites of origin for neuroendocrine chemoreceptor paragangliomas (also known as chemodectomas and glomus tumors) in animals.

Chemoreceptor organs are present in several sites of the body, such as the cartotid body, aortic body, nodose ganglion of the vagus nerve, ciliary ganglion of the orbit, pancreas, jugular vein, middle ear, and glomus jugulare near the glossopharyngeal nerve.[13]

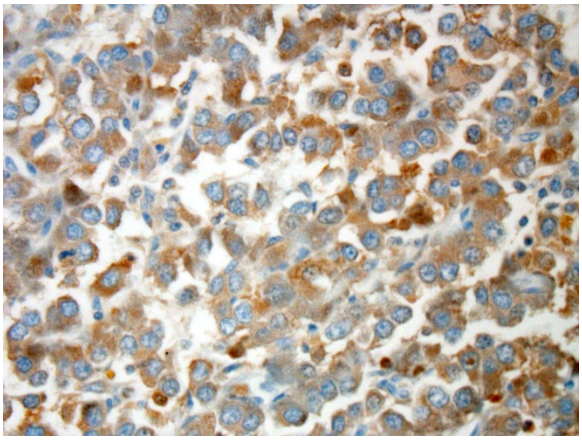

Spleen dog. Neoplastic cells exhibit moderate cytoplasmic immunopositivity for synaptophysin. (anti-synaptophysin, 400X)

As mentioned by the contributor, they are all highly sensitive to changes in blood pH, oxygen tension, and temperature, and can rapidly change respiratory and heart rate via the autonomic nervous system.[13] Metastasis occurs in about 1/3rd of cases of chemodectomas arising from the carotid body, and multicentric neoplastic transformation has been frequently reported in brachiocephalic dogs, possibly because of breed-associated anatomic malformations in the upper respiratory tract resulting in chronic hypoxia.[13]

Neoplastic cells in neuroendocrine tumors contain variable numbers of cytoplasmic secretory granules, best visualized by electron microscopy. Additionally, the number of granules is used to distinguish adenomas, which contain more numerous granules, from carcinomas. In addition, neoplastic cells typically will be immunopositive for chromogranin-A, neuron-specific enolase (NSE), synaptophysin, and S100 protein. Prior to the conference, the JPC performed tissue immunohistochemistry for chromogranin-A, NSE, and synaptophysin. Unfortunately neoplastic cells were immunonegative for all three stains; however, participants speculated the results may be due to suboptimal tissue fixation.[13]

Contributing Institution:
Western University of Health Sciences
College of Veterinary Medicine
Pomona, California 91766
http://www.westernu.edu/veterinary/

References:

1. Aupperle H, März I, Ellenberger C, Buschatz S, et al. Primary and secondary heart tumours in dogs and cats. *J Comp Pathol.* 2007; 136:18-26.
2. Brown PJ, Rema A, Gartner F. Immunohistochemical characteristics of canine aortic and carotid body tumours. *J Vet Med A Physiol Pathol Clin Med*. 2003;50:140-144.
3. Balaguer L, Romano J, Neito JM, Vidal S, Alverez C. Incidental finding of a chemodectoma in a dog: Differential diagnosis. *J Vet Diagn* Invest. 1990; 2:339-341.
4. Capen CC: Endocrine glands. *In*: Maxie MG, ed. *Jubb, Kennedy, and Palmer's Pathology of Domestic Animals*. 5th ed. Vol 3. St. Louis, MO: Elsevier; 2007:425-428.
5. Eriksson, Malin. "Aortic Body Tumors in Dogs." (2011). http://stud.epsilon.slu.se/2545/1/Eriksson_m_110502.pdf
6. Ehrhart N, Ehrhart, EJ, Willis J, Sisson D, Constable P, Greenfield C, Manfra-Maretta S, Hintermeister J. Analysis of factors affecting survival in dogs with aortic body tumors. *Vet Surg*. 2007; 31(1):44-48.
7. Johnson KH. Aortic body tumors in dogs. *J Am Vet Med Assoc*. 1968; 152(2):154.
8. Khodakaram-Tafti A, Shirian S, Shekarforoush SS, Fariman H, Daneshbod Y. Aortic body chemodectoma in a cow: Clinical, morphopathological, and immunohistochemical study. *Comp Clin Pathol*. 2011;20(6):677-679.
9. McManus BM, Allard MF, Yanagawa R. Hemodynamic disorders. In: *Rubin's Pathology: Clinicopathologic Foundations of Medicine*. ed. Rubin R, Strayer DS. 5th ed. Philadelphia, PA: Wolters-Kluwer; 2008:231-232.
10. Noszczyk-Nowak, Agnieszka, Nowak M, Paslawska U, Atamaniuk W, Nicpon J. Cases with manifestation of chemodectoma diagnosed in dogs in Department of Internal diseases with Horses, Dogs and Cats Clinic, veterinary medicine faculty, University of Environmental and Life Sciences, Wroclaw, Poland." *Acta Veterinaria Scandinavica*. 2010; 52:35.
11. Owen TJ, Bruyette DS, Layton CE. Chemodectoma in dogs. *Comp Cont Educ Pract*. 1996;18:253–265.
12. Paltrinieri S, Riccaboni P, Rondena M, Giudice C. Pathologic and immunohistochemical findings in a feline aortic body tumor. *Vet* Pathol. 2004; 41:195-198.
13. Rosol TJ, Grone A. Endocrine glands. In: Maxie MG, ed. *Jubb, Kennedy, and Palmer's Pathology of Domestic Animals*. 6th ed. Vol 3. St. Louis, MO: Elsevier; 2016:354-357.
14. Ware WA, Hopper DL. Cardiac tumors in dogs: 1982–1995. *J Vet Intern* Med. 1995; 13: 95-103.
15. Willis R, Williams AE, Schwarz T, Paterson C, Wotton PR. Aortic body chemodectoma causing pulmonary oedema in a cat. J *Small Anim Pract*. 2001; 42:20-23.

CASE II: 1529704 (JPC 4083862).

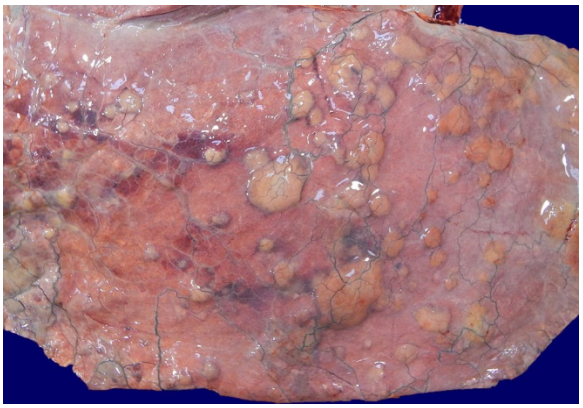

Lung, horse. Numerous 0.5-5cm tan nodules elevate the pleura in all lung fields. (Photo courtesy of: University of Pennsylvania School of Veterinary Medicine, Department of Pathobiology, 4005 MJR-VHUP, 3900 Delancey Street, Philadelphia, PA 19104 http://www.vet.upenn.edu/research/academic-departments/pathobiology)

Signalment: 14-year-old, thoroughbred, gelding, horse, (*Equus caballus*).

History: The patient was admitted for evaluation of chronic colic, and had a distended abdomen on arrival. The horse was diagnosed with uroperitoneum and was euthanized after a tear in the ventral portion of the urinary bladder was confirmed on abdominal ultrasound and cystoscopy. Clinical signs of disease involving other organ systems (*e.g*. respiratory tract) were not reported.

Gross Pathology: The patient was in satisfactory nutritional and good postmortem condition. The peritoneum contained abundant turbid, light-yellow fluid with a distinct ammonia odor *(i.e*. urine), and was hyperemic with adherent plaques of fibrin. The urinary bladder was distended and a 7 x 5 cm thin, gray-green and friable (necrotic) focus within the ventral wall was confirmed. However, examination of the lungs revealed multifocal to coalescing 0.5- 5 cm diameter firm tan nodules that extended into all fields, replacing the pulmonary parenchyma and elevating the visceral pleura (figure 1). Intervening pulmonary parenchyma was pale pink to dark red and mildly firm cranioventrally. The brain, spinal cord, and remainder of the thoracic and abdominal viscera were grossly unremarkable.

Laboratory results: None

Histopathologic Description: Approximately 80% of the pulmonary parenchyma was effaced by multifocal to coalescing nodules composed of proliferating spindle cells (fibroblasts) embedded within a fibrillar eosinophilic (collagenous) stroma, and infiltrated by large numbers of lymphocytes and histiocytes, with fewer neutrophils. Occasionally, alveolar macrophages contained 3-4µm diameter eosinophilic intranuclear inclusion bodies that peripheralized the chromatin (Cowdry Type A inclusions; figure 2 (arrow)). Within affected regions, the majority of alveoli were lined by plump cuboidal epithelial cells (bronchiolization). Affected alveoli, and occasional bronchi and bronchioles, were filled with numerous foamy macrophages, neutrophils, and cell debris. Within

Lung, horse. The submitted section contains several well demarcated nodules which efface the pulmonary parenchyma. (HE, 5X)

unaffected regions of lung, alveoli were often ectatic (hyperinflated), and there was mild multifocal alveolar hemorrhage.

Contributor's Morphologic Diagnoses: Lung: severe chronic multifocal–coalescing sclerosing lymphohistiocytic and neutrophilic bronchointerstitial pneumonia with intrahistiocytic intranuclear inclusion bodies (consistent with equine multinodular pulmonary fibrosis).

Contributor's Comment: Equine multinodular pulmonary fibrosis (EMPF), one of the relatively few differentials for interstitial lung disease in the horse, results in a unique gross and histologic appearance dominated by a nodular pattern of marked interstitial fibrosis.[10] Clinical signs of affected horses may include tachypnea, dyspnea, nasal discharge, coughing, lethargy, inappetence, and poor body condition. Affected horses may have increased bronchovesicular sounds, fever, and/or hypoxemia on clinical exam.[14] Hematology typically reveals a neutrophilia (in some cases with increased bands), lymphopenia or lymphocytosis, and monocytosis.[7,14] A nodular interstitial pattern is often identified on thoracic radiographs and ultrasound, resulting in differential diagnoses of EMPF, fungal pneumonia and pulmonary neoplasia.

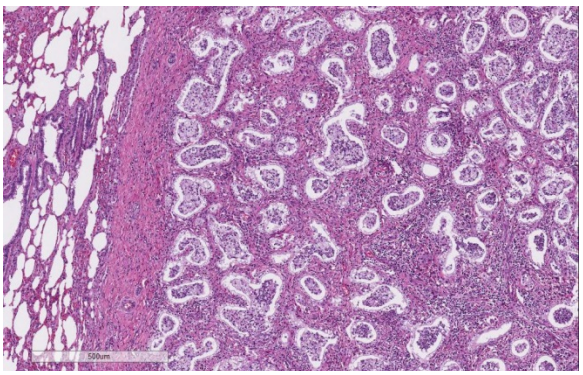

Lung, horse. The nodules are composed of alveolar spaces which are scatted through dense areas of fibrosis and a cellular infiltrate. Each nodule is surrounded by a thick fibrous capsule and compresses the adjacent parenchyma. (HE, 49X)

Concurrent with the interstitial pulmonary disease, thoracic ultrasonography may also reveal pulmonary artery dilation, consistent with pulmonary hypertension. Transtracheal wash fluid is predominantly neutrophilic (degenerate or non-degenerate), with fewer macrophages.[14] No breed or sex predilection has been established, and although affected horses are typically middle-aged or geriatric, cases have been reported in horses as young as four years-old.[12]

Two gross patterns of EMPF have been described, both of which are characterized by multifocal moderately firm, tan, bulging nodules throughout the pulmonary parenchyma. In the more common of the two gross forms (the form exhibited by this horse), these nodules are numerous but small (up to 5 cm in diameter), and coalesce, often resulting in scant intervening parenchyma. In the second gross pattern, the nodules are less frequent, larger (up to 10 cm in diameter), and discrete, with the intervening pulmonary parenchyma largely unaffected.[12] Histologically, both gross forms are characterized by extensive interstitial deposition of mature collagen, accompanied by moderate mixed inflammatory infiltrates, consisting predominantly of lymphocytes, macrophages and neutrophils. Alveoli in affected regions are typically lined by plump, cuboidal epithelium, and airways contain abundant neutrophils and macrophages. Alveolar macrophages occasionally contain amphophilic to eosinophilic intranuclear inclusion bodies. Less frequently, the nodules consist of dense sheets of disorganized collagen that completely efface the normal alveolar pattern.[12]

Equine herpesvirus-5 (EHV-5) is a gamma herpesvirus strongly associated with EMPF, and can be identified by polymerase chain reaction (PCR), immunohistochemistry

(IHC), in situ hybridization, virus isolation, and transmission electron microscopy (TEM).[2,7,12-14] Although causality has not been proven by meeting all of Koch's postulates, the main histologic and immunohistochemical features have been recapitulated in horses inoculated with EHV-5 isolated from EMPF-affected horses.[13] However, because inoculated horses lacked clinical signs associated with EMPF, were PCR-negative for the inoculated EHV-5 viruses (within the lungs), and the virus was unable to be re-isolated, the authors suggest that the immuno-histochemical detection of virus in the inoculated horses having deposition of fibrous connective tissue likely represented a pre-clinical, yet latent, phase of viral infection.[13] Further supporting EHV-5 as an important etiologic factor in the development of EMPF, quantitative real-time PCR performed in an affected horse revealed higher viral load within the lungs than in other tissues, with the highest load within the most severely affected/fibrotic regions of lung.[4] In addition, gamma herpesviruses have been associated with fibrotic lung diseases in other species, including a variably fibrotic broncho-interstitial pneumonia with syncytial cell formation in donkeys associated with asinine herpesvirus-4 and 5 (AHV-4 and 5),[3] and human idiopathic pulmonary fibrosis associated with human herpesvirus-8 (HHV-8) and Epstein-Barr virus.[10,11] Moreover, mice that are knockouts for the IFNγ cytokine receptor (an important mediator of the Th1 antiviral response), develop progressive pulmonary interstitial fibrosis after chronic infection with murine gamma herpesvirus-68.[5,11] Although the precise mechanisms of gamma herpesvirus-induced fibrosis and immune system evasion in most species are unknown, they are likely related to the specific viral-induced cytokine, chemokine, and/or receptor profile within

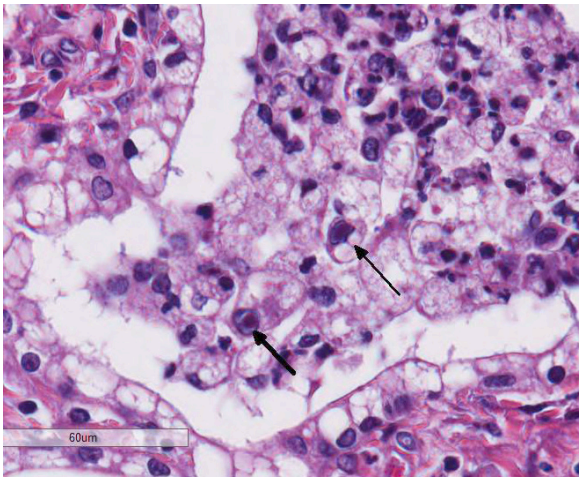

Lung, horse. Remaining alveolar spaces are lined by cuboidal Type II pneumocytes with vacuolated cytoplasm and contain a mixed histiocytic and neutrophilic exudate. Alveolar macrophages occasionally contain a 3-6um eosinophilic intranuclear viral inclusion surrounded by a clear halo. (HE, 400X)

the host, which either directs the immune system toward a Th2 response (thereby inhibiting a Th1 response and facilitating fibrosis), or at least prevents an effective Th1 antiviral response.[6,11] Such mechanisms have already been established in the study of human gamma herpesviruses, including viral CCL-1 (vCCL-1), vCCL-2, and vCCL-3 encoded by HHV-8 that activate Th2 cell chemokine receptors (CCR8, CCR3 and CCR8, and CCR4, respectively), and a viral IL-10 homologue produced by human Epstein-Barr virus that results in inhibition of the Th1 antiviral response.[6,11] In spite of supporting evidence of EHV-5 infection inciting EMPF, EHV-5 may not be the sole cause. As with many infectious diseases, concurrent viral infections (such as EHV-2 and AHV-4 or 5), and the host's immune status, may also be important contributors to the pathogenesis of EMPF.[1,5,11,12]

Although successful treatment with corticosteroid and antiviral (acyclovir) therapy is reported, overall, response to

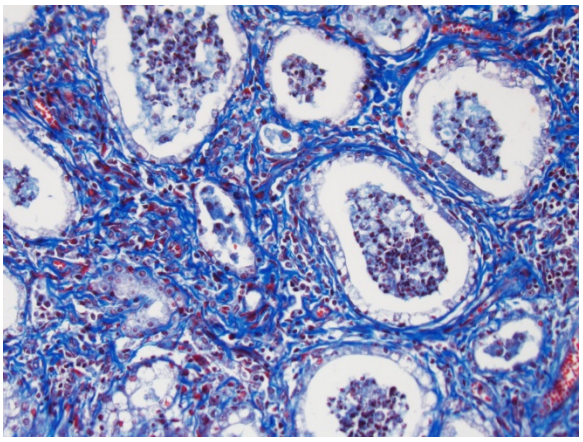

Lung, horse. A Masson's trichrome demonstrates the profound fibrosis which characterizes this lesion. (Masson's, 200X).

treatment is variable and the prognosis of this disease is generally considered poor.[14] This case was unusual in that there were no reported clinical signs that were clearly attributable to respiratory disease. However, a preclinical, latent phase of infection is considered unlikely given the presence of numerous inclusion bodies. Although the uroperitoneum accounted for the most recent episode of colic, it is possible that the pneumonia caused chronic lethargy and inappetence, vague signs that were interpreted as chronic colic. Regional transmural necrosis of the urinary bladder was confirmed histologically, and was attributed to pressure-induced ischemia secondary to distension. As there was no evidence of urethral obstruction, a neurogenic cause was suspected. However, no histologic lesions were identified within the spinal cord.

JPC Diagnosis: Lung: Fibrosis, interstitial, nodular, multifocal to coalescing, severe with lymphohistiocytic interstitial inflammation, alveolar neutrophilic and histiocytic exudate, type II pneumocyte hyperplasia and histiocytic intranuclear viral inclusion bodies, thoroughbred, *Equus caballus*.

Conference Comment: We thank the contributor for both an excellent example and thorough summary of equine multinodular pulmonary fibrosis (EMPF) in horses. This entity has also been extensively reviewed in previous Wednesday Slide Conferences (2011 Conference 1 Case 2, 2012 Conference 24 Case 3, 2013 Conference 18 Case 1), but it was chosen again because of its highly distinctive and unique histomorphology. Participants identified multifocal discrete lung nodules with abundant interstitial fibrosis, marked type II pneumocyte hyperplasia, and irregular alveolus-like spaces filled with an inflammatory exudate composed of neutrophils, fibrin, and alveolar macrophages which occasionally contain a 2-4 um magenta intranuclear inclusion body. Conference participants also noted especially prominent pleural arteries in areas adjacent to the nodules of fibrosis with hypertrophic smooth muscle in the tunica media indicative of pulmonary hypertension associated with pulmonary fibrosis.

As mentioned by the contributor, gamma herpesviruses have been associated with progressive pulmonary fibrotic disorders in humans, donkeys, horses, and rodents. In dogs, canine idiopathic pulmonary fibrosis is a progressive pulmonary fibrotic disorder predominantly in aged West Highland white terriers (WHWT).[9] Recently, investigators have tried to elucidate a relation between this disorder in WHWTs and gamma-herpesvirus infection; however, no evidence a connection was found. Given this condition's predilection for WHWT, it is thought that there is a genetic component to this disease in this breed of dog rather than an infectious etiology.[9]

In addition to pulmonary fibrosis, conference participants discussed the

association of a gamma herpesvirus with retroperitoneal fibromatosis (RF), an aggressive proliferation of highly vascular fibrous tissue subjacent to the peritoneum involving the ileocecal junction and mesenteric lymph nodes in rhesus macaques.[10] RF is associated with co-infection of simian retrovirus 2 (SIV) causing simian acquired immunodeficiency syndrome (SAIDS) and RF-associated herpesvirus (RFHV). This condition is closely related to Kaposi's sarcoma in humans, caused by co-infection of human herpesvirus 8 (HHV8) and human immuno-deficiency virus (HIV), and is one of the first illnesses associated with the development of AIDS.[10] Additionally, rhesus macaque rhadinovirus, another gammaherpesvirus, is also closely related to HHV8 and both have been associated with the development of B-cell lymphoma.[8]

Contributing Institution:

University of Pennsylvania School of Veterinary Medicine
Department of Pathobiology
Philadelphia, PA 19104
http://www.vet.upenn.edu/research/academic-departments/pathobiology

References:

1. Back H, Kendall A, Grandón R, et al. Equine multinodular pulmonary fibrosis in association with asinine herpesvirus type 5 and equine herpesvirus type 5: a case report. *Acta Vet Scand.* 2012;54(57):1-5.
2. Caswell JL, Williams KJ: Equine multinodular pulmonary fibrosis. In: Maxie MG ed. *Jubb, Kennedy, and Palmer's pathology of domestic animals.* Vol 2. 6th ed. St. Louis, Missouri: Elsevier; 2016:568-569.
3. Kleiboeker SB, Schommer SK, Johnson PJ, et al. Association of two newly recognized herpesviruses with interstitial pneumonia in donkeys (*Equus asinus)*. *J Vet Diagn Invest.* 2002;14:273-280.
4. Marenzoni ML, Passamonti F, Lepri E, et al. Quantification of *Equid herpesvirus 5* DNA in clinical and necropsy specimens collected from a horse with equine multinodular pulmonary fibrosis. *J Vet Diagn Invest.* 2011;23(4):802-806.
5. Mora AL, Woods CR, Garcia A, et al. Lung infection with γ-herpesvirus induces progressive pulmonary fibrosis in Th2-biased mice. *Am J Physiol Lung Cell Mol Physiol*. 2005;289:L711-L721.
6. Nicholas J. Human gamma-herpesvirus cytokines and chemokine receptors. *J Interf Cytok Res*. 2005;25:373-383.
7. Niedermaier G, Poth T, Gehlen H. Clinical aspects of multinodular pulmonary fibrosis in two warmblood horses. *Vet Rec.* 2010;166:426-430.
8. Orzechowska BU, Powers MF, et al. Rhesus macaque rhadinovirus-associated non-Hodgkin lymphoma: Animal model for KSHV associated malignancies. *Blood*. 2008; 112:4227-4234.
9. Roels E, Dourcy M, et al. No evidence of herpesvirus infection in West Highland white terriers with canine idiopathic pulmonary fibrosis. *Vet Pathol*. 2016; 53(6):1210-1212.
10. Rose TM, Strand KB, et al. Identification of two homologs of the Kaposi's sarcoma-associated herpesvirus (human herpesvirus 8) in retroperitoneal fibromatosis in different macaque species. *J Virol*. 1997; 71:4138-4144.
11. Tang Y, Johnson JE, Browning PJ, et al. Herpesvirus DNA is consistently detected in lungs of patients with

idiopathic pulmonary fibrosis. *J Clin Microbiol*. 2003;41(6):2633-2640.
12. Williams KJ. Gammaherpesviruses and pulmonary fibrosis: evidence from humans, horses and rodents. *Vet Pathol*. 2014;51(2):372-384.
13. Williams KJ, Maes R, Del Piero F, et al. Equine multinodular pulmonary fibrosis: a newly recognized herpesvirus-associated fibrotic lung disease. *Vet Pathol*. 2007;44:849-862.
14. Williams KJ, Robinson NE, Lim A, et al. Experimental induction of pulmonary fibrosis in horses with gammaherpesvirus Equine Herpesvirus 5. *PLoS ONE*. 2013;8(10):e77754, doi. 10.1371/journal.pone.0077754.
15. Wong DM, Belgrave RL, Williams KJ, et al. Multinodular pulmonary fibrosis in five horses. *J Am Vet Med Assoc*. 2008;232(6):898-905.

CASE III: CAN2 (JPC 4084949).

Signalment: Nine-year-old, female, golden retriever, (*Canis familiaris*).

History: The dog was brought to the clinic with a history of intermittent rectal prolapse. Clinical examination revealed a rectal mass (5 cm cranial from the anus), and the dog was referred to the surgical excision of the mass.

Gross Pathology: Rectal mass: an oval 3x5 cm mass, on cross section light brown in color and firm consistency.

Laboratory results: Immunohisto-chemistry – antibodies against CD 3, CD79 and MUM1 were applied. The tumor was CD79 and MUM1 positive, and CD3 negative. Congo red stain revealed amyloid deposits at the periphery of the tumor.

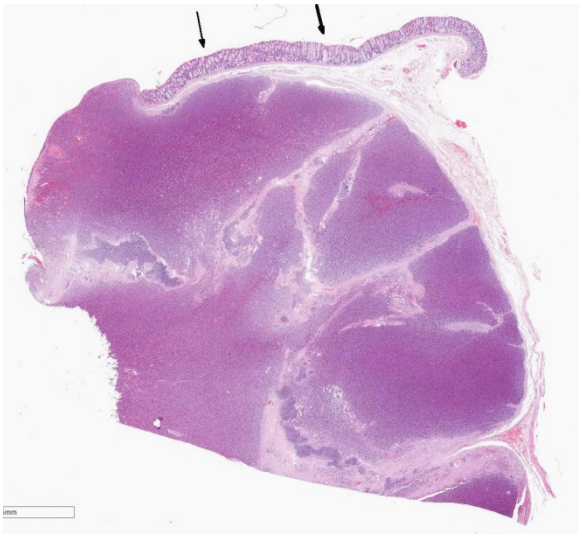

Rectum, dog. Within the wall of the rectum, there is a well-demarcated infiltrative mass that transmurally effaces the colonic wall. The overlying intact mucosa is delineated by arrows. (HE, 4X)

Histopathologic Description: Rectum: Expanding the submucosa and elevating the overlying ulcerated mucosa is a well circumscribed, partially encapsulated, densely cellular neoplasm composed of sheets and packets of round cells separated by a fine fibrous stroma. Neoplastic cells have variably distinct cell borders and moderate amounts of eosinophilic granular cytoplasm. Nuclei are round, rarely oval, usually eccentrically located with finely stippled to finely clumped chromatin and usually one indistinct nucleolus. There is moderate anisokaryosis, multifocal karyo-megaly and a moderate number of multinucleate cells. Mitotic figures average 10 per 10 HPF. Multifocally between neoplastic cells or at the periphery of the tumor are variably sized and shaped, extracellular deposits of amorphous, homogenous, eosinophilic material (amyloid) with multifocal islands of cartilage formation (cartilaginous metaplasia) that is occasionally mineralized.

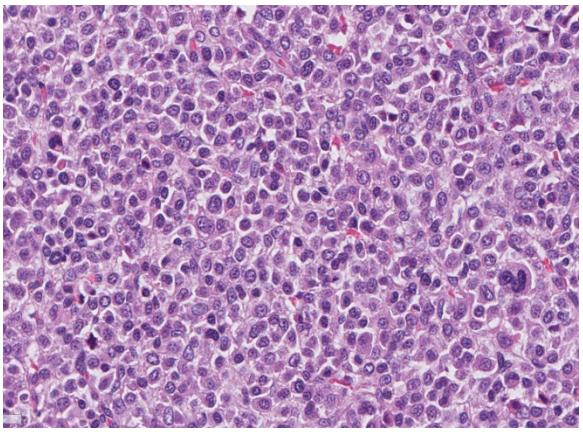

Rectum, dog. Neoplastic cells are round and arranged in poorly-defined nests and packets. Neoplastic cells have eccentric, occasionally helmet-shaped nuclei, are occasionally multinucleate, and exhibit moderate anisocytosis and anisokaryosis. (HE, 400X) (Photo courtesy of: Department of Veterinary Pathology, Faculty of Veterinary Medicine, University of Zagreb, Heinzelova 55, 10000 Zagreb, Croatia. http://www.vef.unizg.hr/)

Contributor's Morphologic Diagnoses: Rectum: Plasmacytoma (or Extramedullary Plasmacytoma), golden retriever, canine.

Contributor's Comment: Extramedullary plasmacytoma (EMP) is a relatively common tumor in older dogs and occur most frequently on the skin and mucous membranes, but has been reported in other areas such as the brainstem, spinal cord, lymph nodes, abdominal viscera, genitalia, and eyes.[2,9]

Plasmacytomas of the lower gastrointestinal tract are uncommon neoplasms in dogs, and rare in cats and other species. They are encountered most frequently in the submucosa of the distal colon and rectum of dogs, where they are associated with signs of large bowel diarrhea and bleeding[5]. Gastrointestinal EMP has also been reported in other sites, including the esophagus, stomach and small intestine.[10]

Histologically they resemble plasmacytomas of the skin, oral cavity or larynx. The tumor is formed by solid packets of pleomorphic round cells with various degrees of plasmacytoid maturation, especially at the periphery of the tumor. There is a frequent nuclear hyperchromasia and convolution. The cells are typically arranged in solid endocrine-like packets and there may be AL amyloid deposition among the tumor cells. The majority of the tumor growth is submucosal. A small proportion exhibit more aggressive behavior, including invasion of tunica muscularis, and some spread to regional lymph nodes and spleen.[9] Canine EMP histological typing system has been established and is helpful diagnostic tool, although the types cannot be used for a tumor grading system.[4]

An unusual finding in plasmacytomas is the presence of cartilage and bone in close association with amyloid deposits. Meta-plastic bone and cartilage have been described in two canine intestinal EMPs[5] and in human amyloidosis of tongue[11] and myelomas.[1] The exact pathogenesis of chondroid metaplasia in amyloidosis is not clearly described. Ramos Vara and colleagues hypothesized that in amyloidosis the inducing stimulus for bone formation is

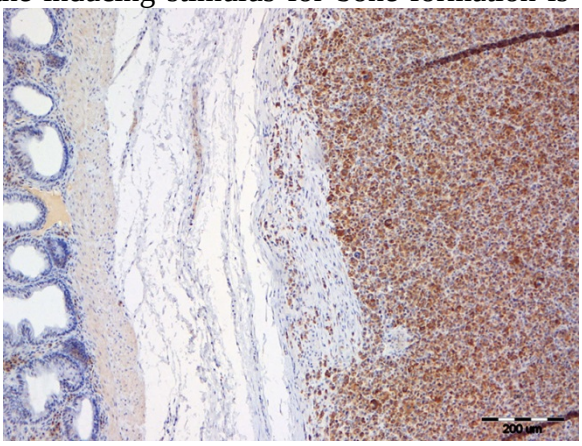

Rectum, dog. Neoplastic cells display strong membranous immunopositivity for CD-79. (anti-CD79, 100X)

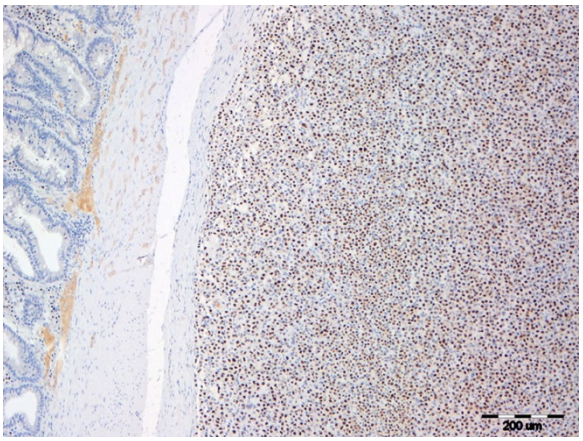

Rectum, dog. Neoplastic cells display strong nuclear immunopositivity for MUM-1. (anti-MUM1, 100X)

the amyloid deposits, with resultant stimulation of mesenchymal precursor cells to differentiate into cartilage- and bone-forming cells under the influence of soluble factors liberated by histiocytic and other cells.[5]

JPC Diagnosis: Colon: Plasmacytoma, extramedullary, golden retriever, *Canis familiaris*.

Conference Comment: The contributor provides a great example of a relatively common neoplasm in the skin or mucus membrane of dogs in an uncommon location within the abdominal viscera. Extra-medullary plasmacytomas of the lower gastrointestinal tract have been reported in dogs to occur most frequently in the submucosa of the distal colon and rectum, as in this case, and are considered a benign neoplastic proliferation of monoclonal B cells.[9] Rectal and colonic plasmacytomas represent only 4% of all extramedullary plasmacytomas in dogs.[6] Despite the uncommon location, conference participants identified solid packets of pleomorphic plasmacytoid round cells with a perinuclear clearing (Golgi complex) admixed with abundant homogenous smudgy material recognized as amyloid, commonly deposited in plasma cell tumors. The contributor confirmed the presence of amyloid via Congo-red staining and apple-green birefringence with polarized light. The conference moderator also pointed out the distinctive clumping pattern of the hetero-chromatin, giving the neoplastic cells the classic "clock face" histomorphology of plasma cells.[9]

The most striking feature of this case is the prominent streaks of amyloid within and surrounding the neoplasm, often admixed with foci of chondroid metaplasia. Amyloid is a proteinaceous substance composed of polypeptides arranged in beta-pleated sheets and is deposited in tissues in response to a number of pathogenic processes. Primary systemic or immunoglobulin associated amyloid (AL) is associated with light chains derived from plasma cells in monoclonal B cell proliferations of extramedullary plasmacytomas or multiple myelomas. The light chains are then converted to amyloid fibrils by proteolytic enzymes in macro-phages and deposited within tissues.[8] As mentioned by the contributor, chondroid metaplasia has been uncommonly reported to occur with amyloidosis secondary to a

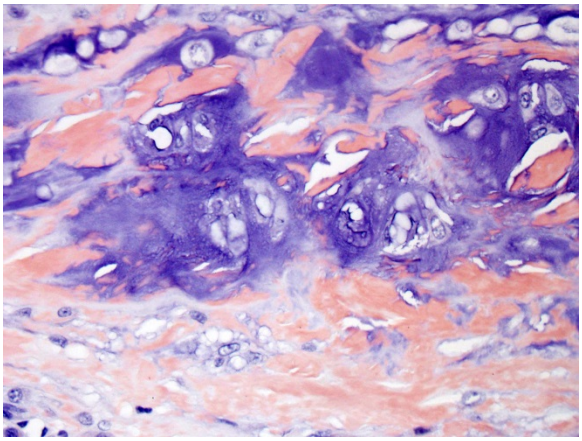

Rectum, dog. Scattered through the neoplasm are aggregates of congophilic amyloid protein which contain numerous well-differentiated chondrocytes encased in a bluish cartilaginous matrix. (Congo Red, 400X)

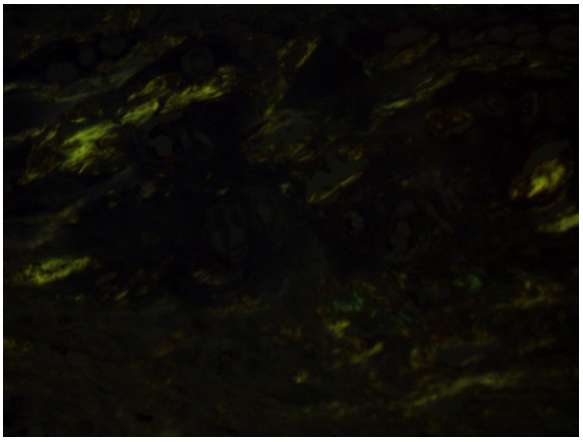

Rectum, dog. Lakes of amyloid exhibit distinct apple-green birefringence when illuminated with polarized light. (Congo Red, 400X).

variety of conditions, although the exact pathogenesis is currently unknown.[3,11]

Another type of amyloid is formed secondary to a variety of chronic inflammatory conditions inciting excessive release of serum amyloid associated (AA) acute phase protein, predominantly by the liver under the influence of interleukin-6 (IL-6) and IL-1. AA is then deposited in multiple organs including the spleen, pancreas, intestinal lamina propria, lymph nodes, kidneys and liver.[7,8,9] Amyloid-beta (AB) has been found in cerebral plaques of aging humans and rhesus macaques and is associated with Alzheimer's disease. Interestingly, neurofibrillary tangles, another feature of Alzheimer's disease in humans, have not been found in aging rhesus macaques.[7]

Contributing Institution:

Department of Veterinary Pathology
Faculty of Veterinary Medicine
University of Zagreb
10000 Zagreb
Croatia.
http://www.vef.unizg.hr/

References:

1. Karasick DV, Schweitzer ME, Miettinen M, O'Hara BJ. Osseous metaplasia associated with amyloid-producing plasmacytoma of bone: A report of two cases. Skeletal Radiol. 1996; 25:263–267.
2. Jacobs JM, Messick JB, Valli VE. Lymphoid Tumors. In: Meuten DJ, ed. *Tumors in Domestic Animals*. 4th ed. Iowa State Press; Blackwell Publishing; 2002: 163.
3. Gross TL, Ihrke PJ, Walder EJ, Affolter VK. *Skin Diseases of the Dog and Cat*. 2nd ed. Ames, IA: Blackwell; 2005: 870-871.
4. Platz SJ, Breuer W, Pfleghaar S, Minkus G, Hermanns W. Prognostic value of histopathological grading in canine extramedullary plasma-cytomas. *Vet Pathol*. 1999; 36: 23-27.
5. Ramos-Vara JA, Miller MA, Pace LW, Linke RP, Common RS, Watson GL. Intestinal multinodular AL deposition associated with extramedullary plasmacytoma in three dogs: Clinicopathological and immunohistochemical Studies. *J Comp Path.* 1998; 119: 239-249.
6. Rannou B, Helie P, Bedard C. Rectal plasmacytoma with intracellular hemosiderin in a dog. *Vet Pathol*. 2009; 46:1181-1184.
7. Simmons HA. Age-associated pathology in rhesus macaques (*Macaca mulatta*). *Vet Pathol*. 2016; 53(2):399-416.
8. Snyder PW. Diseases of immunity. In: McGavin MD, Zachary JF, ed. *Pathologic Basis of Veterinary Disease*, 6th ed. St Louis, MO: Elsevier Mosby; 2017:285.
9. Uzal FA, Plattner BL, Hostetter JM. Alimentary system. In: Maxie MG, ed. *Jubb, Kennedy, and Palmer's Pathology of Domestic Animals*. 6th

ed. Vol 2. St. Louis, MO: Elsevier; 2016:109.
10. Vail DM. Plasma Cell Neoplasms. In: Withrow SJ, Vail DM, eds. *Small Animal Clinical Oncology*. 4th ed. Philadelphia, PA: Elsevier Saunders; 2007: 769-784.
11. Vasudevan JA, Somanathan T, Patil SA, Kattoor J. Primary systemic amyloidosis of tongue with chondroid metaplasia. *J Oral Maxillofac Pathol*. 2013; 17(2): 266-268.

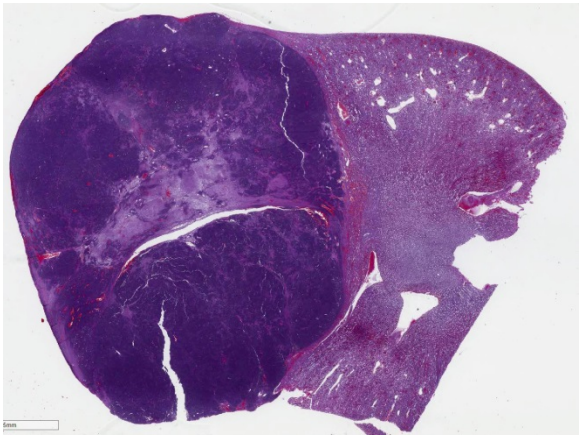

Kidney, rabbit. At one pole of the kidney, there is a densely cellular, nodular, expansile neoplasm. (HE, 5X)

CASE IV: E-522/16 (JPC 4088269).

Signalment: Three-year-old male rabbit (*Oryctolagus cuniculus*).

History: The animal presented two days of anorexia and lack of defecation. At physical examination, a single mass was detected by palpation at the right lumbar area. The presence of a round-shaped mass associated to the caudal pole of the right kidney was confirmed by ultrasonography. Clinicians suspected a neoplastic process, and a right nephrectomy was performed.

Gross Pathology: The complete right kidney was submitted for histopathologic evaluation. A well-circumscribed, oval white mass, 2x1.5 cm in diameter was observed at the caudal pole of the kidney. On section, its consistency was soft, and the cut surface was white and homogeneous.

Laboratory results: None

Histopathologic Description: Kidney: Replacing 50-75% of the renal tissue, there is a densely cellular, partially encapsulated but infiltrative nodular neoplasm which compresses adjacent parenchyma. The neoplasm is composed of a disorganized mixture of epithelial, mesenchymal, and blastemal components supported by an abundant fibrovascular stroma which, in some areas, is embedded in a loose, pale eosinophilic, collagenous matrix. The mesenchymal and blastemal components are predominant over the epithelial. Epithelial neoplastic cells are cuboidal to cylindrical and arranged in a tubular pattern. Occasionally, there are very scant tuft invaginations into the tubular lumen lined by flat epithelial cells (primitive glomerular structures). Those cells present well-defined cytoplasmic borders and moderate amount of bright eosinophilic cytoplasm. Nuclei are round, irregularly shaped, mostly basally located, with grossly stippled chromatin and less frequently, finely stippled chromatin with one basophilic nucleolus. There is low-grade anisokaryosis and anisocytosis, and low mitotic index (1/40X HPF). The mesenchymal component is arranged in a storiform pattern or disorganized bundles. Cells are fusiform, with an indistinct cytoplasmic border, scant eosinophilic cytoplasm, and fusiform centrally located nuclei with grossly stippled chromatin. There is a mild anisokaryosis and aniso-cytosis, and a low mitotic index (0-1/40X HPF). Some of these cells, organized in nest or ribbons, which are poorly differentiated

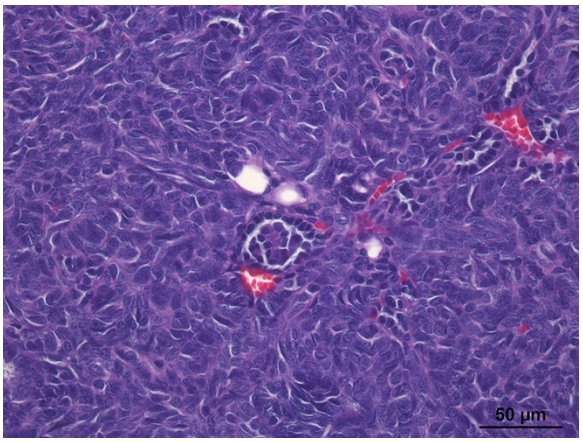

Kidney, rabbit. The neoplasm is composed of spindled to polygonal cells arranged in short streams which occasionally form tubules with papillary projections within, interpreted as "glomeruloid" structures. (HE, 400X) (Photo courtesy of: Servei de Diagnostic de Pathologia Veterinaria, Facultat de Veterinaria, Barcelona 08193, SPAIN)

are identified as possible blastemal cells. Multifocally, in the neoplastic mass there are areas of hypereosinophilia and loss of cytoplasmic and nuclear detail (coagulative necrosis) and mild lymphoplasmacytic inflammatory infiltrate is observed among the neoplasia. The adjacent renal parenchyma shows a moderate interstitial fibrosis, and intense congestion.

Contributor's Morphologic Diagnoses: Renal nephroblastoma.

Contributor's Comment: Nephroblastoma, or Wilms´ tumor, is the most common primary renal tumor of pigs and chickens, and occurs far less often in calves and dogs. It is frequently observed in young animals, although it may be seen in mature sows, and is more common in adult dogs than in pups. Clinically, it is usually an incidental finding except in dogs, in which some animals present with spinal dysfunction as result of compression of the spinal cord associated with neoplastic infiltration into the vertebral canal. Macroscopically, it is usually a solitary unilateral mass located at one pole of the kidney, but it can be multiple and/or bilateral. Nephroblastoma is a true

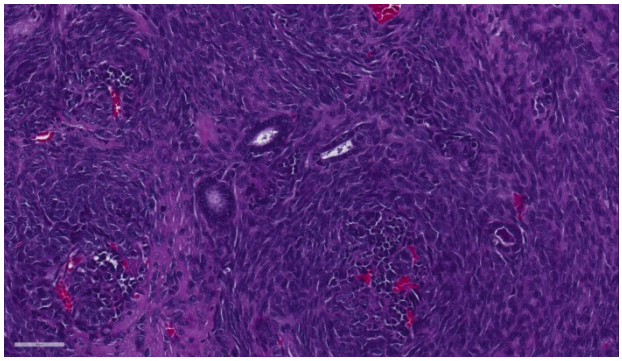

Kidney, rabbit. Neoplastic cells also often form well-differentiated tubules. (HE, 400X)

embryonal tumor that arises from primitive metanephric blastema and exhibits blastemal, epithelial, and stromal components in variable proportions. Histologically, it is characterized by the presence of primitive glomeruli, abortive tubules, and loose spindle-cell stroma that may differentiate into a variety of mesenchymal tissues.

Tubular and glomerular differentiation indicate a good prognosis, whereas anaplasia and sarcomatous stroma are associated with metastasis and a poor prognosis. In this case, the epithelial component is scant and poorly differentiated, and there is a clear predominance of undifferentiated mesenchymal cells. These features, in combination with the neoplasm's invasive growth pattern, suggest a poor prognosis.

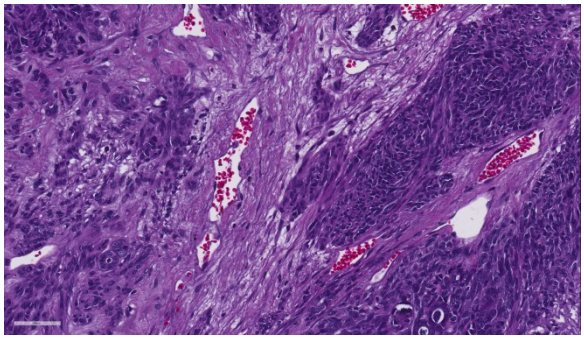

Kidney, rabbit. There are extensive areas of necrosis throughout the neoplasm. (HE, 400X)

The differential diagnosis for renal neoplasia in a rabbit includes renal carcinoma and renal lymphosarcoma. To confirm the diagnosis of nephroblastoma, immunohistochemistry was performed against Wilm's tumor suppressor gene1 (WT1), which has proven efficacious in dogs. This immunohistochemistry was kindly provided by Dr. Joan Carles Ferreres, head of the Pathology Department at the Parc Taulí Sabadell University Hospital. In this case, positive nuclear immunoreactivity was observed in the mesenchymal and blastemal components, as well as endothelial cells.

JPC Diagnosis: Kidney: Nephroblastoma, rabbit, *Oryctolagus cuniculus*.

Conference Comment: This case nicely demonstrates the blastemal, epithelial, and stromal components histologically characteristic for nephroblastomas. Conference participants readily identified the presence of scattered primitive glomeruli (formed by infolded papillary projections of polygonal cells within tubule lumina), as well as low numbers of tortuous, abortive tubules admixed with numerous blastemal cells and surrounded by an abundant loose spindle-cell stroma. Additionally, attendees noted several individualized well-differentiated renal tubules scattered throughout the neoplasm. Conference participants agreed that these likely represent entrapped non-neoplastic renal tubules within the neoplastic cell population rather than part of the epithelial component of the neoplasm. There is moderate slide variability, affecting the proportion of the three components present. When all three cell types are present in equivalent proportions, the neoplasm is referred to as triphasic or mixed;[7] however, in this case there appears to be a preponderance of spindle-cell stromal and blastemal components. Although not a prominent feature in this case, the spindle-cell stroma can occasionally differentiate into various types of mesenchymal tissue, such as striated muscle, collagen, adipose tissue, bone, or cartilage.[6,7]

Nephroblastoma rarely causes clinical signs, although polycythemia is an infrequently reported paraneoplastic syndrome in rabbits.[2] The vast majority of nephroblastomas are considered incidental findings and are noted during necropsy as a solitary (or occasionally bilateral) renal masses.[1] However, as mentioned by the contributor, when this neoplasm is characterized predominantly by a poorly differentiated sarcomatous stromal component, as in this case, it tends to metastasize to the lung and liver, portending an overall poor prognosis.[7]

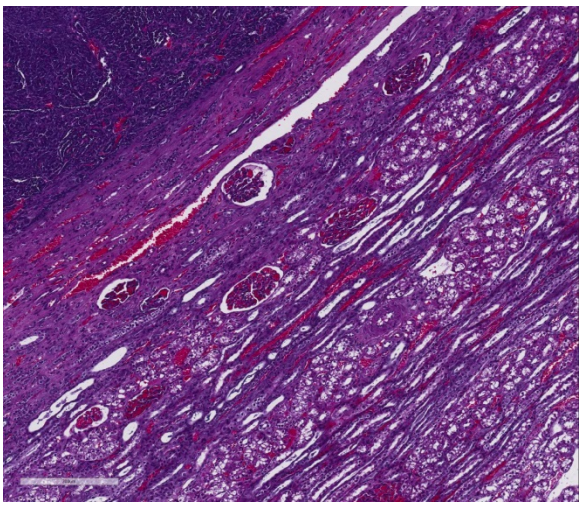

Kidney, rabbit. Growth of the neoplasm (upper left) has resulted in compression of the surrounding cortex and formation of a compression capsule.

While nephroblastomas are a relatively uncommon spontaneous neoplasm in pet rabbits, they can be rapidly induced at a high frequency in laboratory rabbits and rats after exposure to direct-acting alkylating carcinogens, such as dimethylnitrosamine.[6] Dimethylnitrosamine has also been reported to experimentally induce triphasic nephroblastomas in rainbow trout, similar to Wilm's tumor in humans.[3] Other than

lymphoma, nephroblastomas are the most common primary renal neoplasm in a variety of species of freshwater fish, with the Japanese eel over-represented. Research is ongoing to determine if potential carcinogens in the water may be inducing nephroblastomas in wild fish, with a particular focus on fish commonly consumed by people.[3]

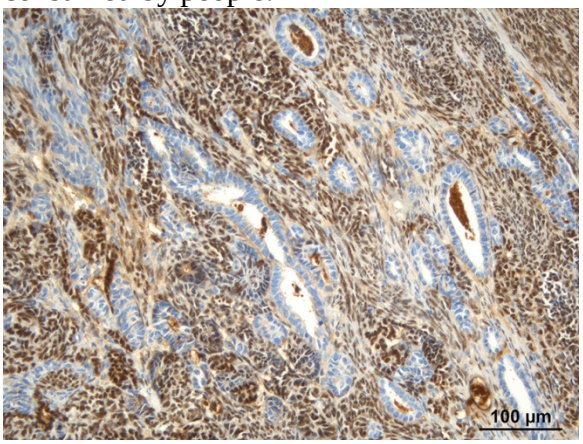

Kidney, rabbit. Neoplastic cells exhibit strong nuclear immunopositivity for Wilm's Tumor 1 (antigen). (anti-WT1, 400X)

Contributing Institution:
Universitat Autonoma de Barcelona
Servei de Diagnostic de Patologia Veterinaria
Barcelona, Spain
http://www.uab.cat/veterinaria/english

References:

1. Cianciolo RE, Mohr FC. The urinary system. In: Maxie MG ed. *Jubb Kennedy and Palmer's Pathology of Domestic Animals*. Vol 2. 6th ed. Philadelphia, PA: Elsevier Saunders; 2016:446-447.
2. Cooper TK, Griffith JW, et al. Spontaneous lung lesions in aging laboratory rabbits (*Oryctolagus cuniculus*). *Vet Pathol*. 2017; 54(1):178-187.
3. De Lorenzi D, Baroni M, Mandara MT. A true "triphasic" pattern: Thoracolumbar spinal tumor in a young dog. *Vet Clin Pathol*. 2007; 36:200-203.
4. Hassan J, Katic N, et al. Treatment of nephroblastoma with poly-cythemia by nephrectomy in a rabbit. *Vet Rec*. 2012; 170:465.
5. Lombardini ED, Hard GC, Hashbarger JC. Neoplasms in the urinary tract in fish. *Vet Pathol*. 2014; 51(5):1000-1012.
6. Meuten DJ. Tumours of the urinary system. In: Meuten DJ, ed. *Tumors in Domestic Animals*. Ames, IA: Iowa State Press; 2002:519-520.
7. Newman SJ. The urinary system. In: McGavin MD, Zachary JF, ed. *Pathologic Basis of Veterinary Disease*. 5th ed. St Louis, MO: Elsevier Mosby; 2012: 643.